ACS Medicinal Chemistry Letters



Letter

# Folate Receptor Targeting and Cathepsin B Sensitive Drug Delivery System for Selective Cancer Cells Death and Imaging

Xiangmei Jin, Jun Zhang, Xiaoyan Jin, Lan Liu, and Xizhe Tian

*ACS Med. Chem. Lett.*, **Just Accepted Manuscript** • DOI: 10.1021/acsmedchemlett.0c00031 • Publication Date (Web): 18 May 2020



## Just Accepted



is published by the American Chemical Society. 1155 Sixteenth Street N.W., Washington, DC 20036

# Folate Receptor Targeting and Cathepsin B Sensitive Drug Delivery System for Selective Cancer Cells Death and Imaging

Xiangmei Jin†, Jun Zhang‡, Xiaoyan Jin†, Lan Liu‡*, and Xizhe Tian†*

†Department of Chemistry, Yanbian University, Yanji 133000, Jilin, China

‡Department of Pathology, Affiliated Hospital of Yanbian University, Yanji 133000, Jilin, China

*Supporting Information Placeholder*

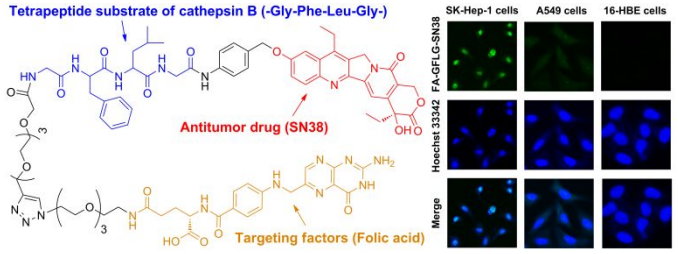


**ABSTRACT:** Folate receptor (FR)-mediated dual-targeting drug delivery system are synthesized to improve tumor-killing efficiency and inhibit the side-effects of anticancer drugs. In this paper, we designed and synthesized FR-mediated fluorescence probe (FA-Rho) and FR-mediated cathepsin B sensitive drug delivery system (FA-GFLG-SN38). FA-GFLG-SN38 is composed of ligand (folic acid, FA) of folate receptor (FR), tetrapeptide substrate (-GFLG-) for cathepsin B and an anticancer drug (SN38). FA-Rho is suitable for specific fluorescence imaging of SK-Hep-1 cells to overexpress FR, and inactive in FR negative A549 and 16-HBE cells. FA-GFLG-SN38 exhibited strong cytotoxic against FR-overexpressed SK-Hep-1, HeLa and Siha cells with $IC_{50}$ of 2-3 μM, with no effects on FR negative A549 and 16-HBE cells. The experimental results show that FA-CFLG-SN38 drug delivery system proposed by us could effectively inhibit tumor proliferation *in vitro*, it can be adopted for the diagnostics of tumor tissues and provide a basis for effective tumor therapy.

**KEYWORDS:** Drug delivery system; Folate receptor; Cathepsin B; Rhodamine B; SN38

Tumor tissues are distinguished from normal by atypical growth, metabolic disorders, aberrant gene expression, and abnormal expression and activity of related enzymes in itself and surroundings.[1] These characteristics lead to abnormal proliferation and metastasis, as well as weaken the antitumor efficacy of conventional treatments. [2] Ehrlich was the first to put forward the option of targeted drug therapy for improving diagnosis and treatment of malignant tumors.[3] An ideal drug delivery system distributes antitumor drugs specifically to target cells, tissues or organs to achieve selective drug delivery, controlled release, and toxicity reduction.[4,5] Tumor receptor-mediated targeted therapies include those involving folate receptor (FR),[6] epidermal growth factor receptor,[7] sialic acid glycoprotein receptor,[8] glycyrrhetinic acid receptor,[9] and transferrin receptor systems.[10] In contrast to lightly expressed in normal tissues, FR is over two orders of magnitude higher expressed on the surface of tumor cells such as ovarian cancer and colon cancer.[11] FA selected as the raw material for the synthesis for tumor-targeting drug delivery systems, due to its characteristics of relatively low cost, non-toxicity, low immunity, stability and easy modification. Xu et al. prepared a glutathione-responsive prodrug based on FA and camptothecin (CPT) *via* disulfide bonds. The resulting FA-CPT prodrug showed higher specificity and cytotoxicity in FR-positive KB tumor cells rather than FR-negative A549 tumor cells.[12] Therefore, FR-mediated active drug delivery system could improve cancer-targeting ability and reduce the side-effects of anticancer drugs.[13]

7-Ethyl-10-hydroxycamptothecin (SN38) is an active metabolite of irinotecan,[14] and also the substrate of p-glycoproteins, multidrug resistance-associated proteins 2 and breast cancer resistance protein efflux pumps.[15] SN38 exerts strong inhibitory activity on DNA topoisomerase I with 100-1000 times greater than irinotecan in cytotoxicity, [16] and it is used as an anticancer drug against malignant tumors *in vitro*[17], such as colorectal, lung, lymphoma, gastric, cervical, and ovarian cancers.[18,19] Its clinical application is limited, however, by poor water solubility and instability.[20] The water solubility of SN38 could be improved through several modifications, including liposome formulation[21], antibody drug conjugates[22], and PEG functionalization[23]. Currently, several delivery systems for irinotecan and its active metabolite SN38 have been developed, and the delivery system of liposome preparation SN38 (LE-SN38) has been studied in clinical trials.[24] LE-SN38 has been evaluated for mCRC following oxaliplatin progression in phase ii studies, and the results

showed that LE-SN38 had acceptable toxicity, but its therapeutic activity can not reach the prescribed criteria. Therefore, the development of an effective SN38 drug delivery system has important clinical significance.

Existing types of tumor microenvironment stimulation include responses to pH, reduction, oxidation, and enzymes.[25-27] Tumor tissues generate abnormal expression or activity of specific enzymes, such as matrix metalloproteinases,[28] cytosolic phospholipase A2,[29] and cathepsin B (CTSB).[30] CTSB as a potential marker for tumor screening and treatment target, has attracted extensive research attention in recent year. The protease specifically hydrolyzes peptides, such as Leu-Leu, Arg-Arg, Ala-Leu, Phe-Arg, Phe-Lys, Gly-Phe-Leu-Gly, and Ala-Leu-Ala-Leu et al,[31, 32] Gly-Phe-Leu-Gly (-GFLG-) is the most commonly used CTSB-responsive substrate among them. Leveraging significant differences in the concentrations and activities of enzymes between tumor and normal tissues, effective enzyme-responsive antitumor drug delivery systems based on the high selectivity of enzymes can be developed.[33]

In order to improve the imaging method and tumor selectivity of treatment, we designed FR-mediated dual-targeting delivery system that could target cancer cell more accurately. FA-$N_3$ was coupled to form the ligand component of FR. The antitumor drug SN38, tetrapeptide chain -GFLG-, and oligoethyleneglycol tether were used to form the drug component. The ligand and drug underwent click reactions to generate the FA-GFLG-SN38 dual-targeted delivery system. Compared with SN38, our system has a number of advantages: 1) FA plays a targeting role in drug-specific guidance to FR-positive cancer cells;[11] 2) CTSB, which is overexpressed in cancer cells, is used to release SN38 under conditions of weak acidity to improve selectivity and reduce the side-effects of antitumor drugs;[30] 3) a relatively long oligoethyleneglycol tether increases the solubility of drugs, allowing longer circulation owing to reduction in renal clearance, enzymatic degradation and immune cell recognition of drugs.[23] We anticipated that SN38 is inactive when linked to the FR-mediated delivery system. The FA-GFLG-SN38 drug delivery system binds to FR on the surface of cancer cells, and it is internalized into cells via FR-mediated endocytosis. Then, the drug released via a 1,6-elimination process and become active within the cells when the C-terminus of the tetrapeptide chain(-GFLG-) in the system cleaved by cancer cells overexpressing CTSB, thus resuming therapeutic activity. In addition, the FA-Rho fluorogenic probe without a CTSB-responsive tetrapeptide was prepared. Although non-cleavable conjugate internalized into cells via FR-mediated, and rhodamine B (Rho) would be accumulated in lysosomes due to the lack of a tetrapeptidic substrate of CTSB. In the research described below, we synthesized and explored the effectiveness of the dual target delivery system. The results suggest that the new dual-target delivery system can indeed be used to selective killing or image cancer cells.

A schematic representation of FA-GFLG-SN38 synthesis is shown in Scheme 1A. Alkyne-linked peptides (alkyne-Gly-Ph e-Leu-Gly) possessing a C-terminal hydrazide were assembled

**Scheme 1.** Synthesis of (A) FA-GFLG-SN38 and (B) FA-Rho.

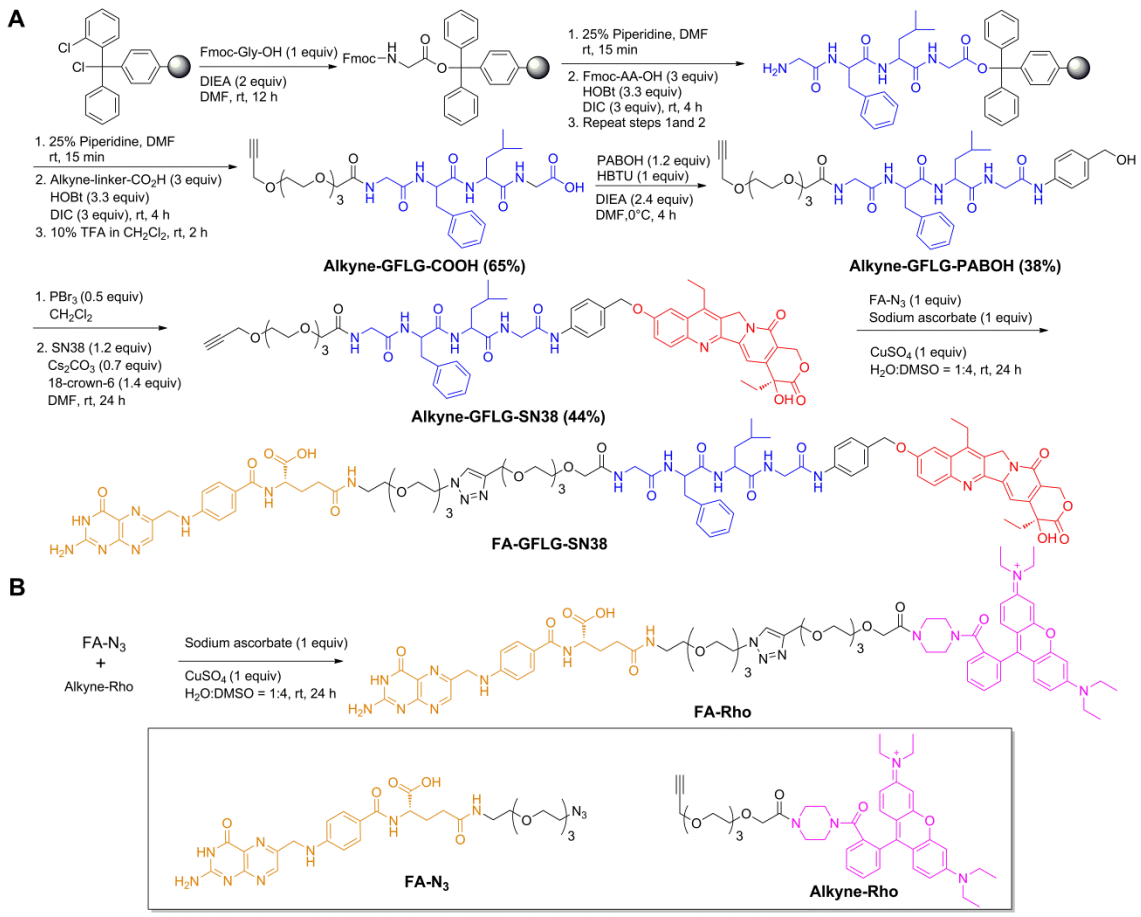

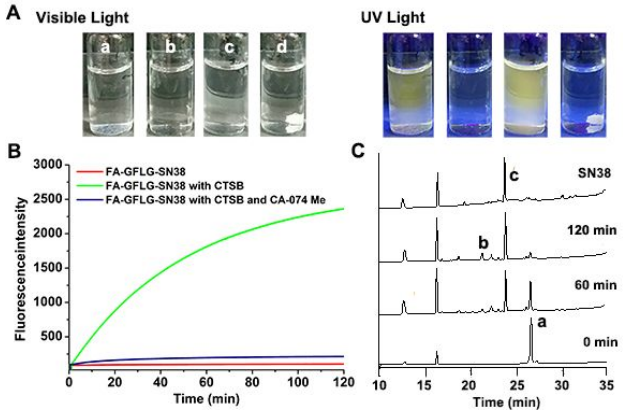


**Figure 1.** Release of the SN38 drug from FA-GFLG-SN38 promoted by CTSB. (A) The images of different solutions (a: SN38; b: FA-GFLG-SN38; c: FA-GFLG-SN38 with CTSB; d: FA-GFLG-SN38 with CTSB and CA-074 Me) under visible light and UV irradiation. (B) Release of SN38 from FA-GFLG-SN38 monitored using a fluorometer ($\lambda_{ex}$ = 365 nm, $\lambda_{em}$ = 540 nm). (C) Release of SN38 from FA-GFLG-SN38 in the presence of CTSB monitored using RP-HPLC (detection at 254 nm) and Mass (a = FA-GFLG-SN38, b = FA-linker-Gly-Phe-OH ([M + Na]: m/z = 1114.7), c = SN38).

on a solid support in the presence of 1-hydroxybenzotriazole (HOBt), diisopropylethylamine (DIEA) and *N,N′*-diisopropylcarbodiimide (DIC). Assembled alkyne-linked peptides were released from the solid support by treatment with 10% trifluoroacetic acid (TFA) in $CH_2Cl_2$. The alkyne-linked peptides and 4-aminobenzyl alcohol (PABOH) formed an amide group. Bromination of the hydroxyl group of alkyne-GFLG-PABOH, followed by nucleophilic substitution and binding of SN38 yielded alkyne-GFLG-PAB-SN38. FAγ-COOH had less steric hindrance compared to α-COOH and could be selectively activated by controlling the molar ratio of FA and *N,N′*-dicyclohexylcarbodiimide (DCC). FA-$N_3$ was obtained via formation of an amide bond with $NH_2$-linker-$N_3$ at a FA:DCC ratio of 1:1.[34] The resulting mixture was purified using semi-preparative reversed-phase high performance liquid chromatography (RP-HPLC) and lyophilized. The retention time of FA-$N_3$ on analytical RP-HPLC was 19.2 min and comparison of peak areas disclosed 74.58% FAγ-coupling. The alkyne-GFLG-SN38 was reacted with FA-$N_3$ under click conditions ($CuSO_4$ and sodium ascorbate), purified with semi-preparative HPLC and lyophilized. The retention time of FA-GFLG-SN38 was 25.44 min on analytical RP-HPLC.

The synthetic pathway of FA-Rho is presented in Scheme 1B. Alkyne-Rho and reacted with FA-$N_3$ under click conditions ($CuSO_4$ and sodium ascorbate). The resulting mixture was purified with semi-preparative RP-HPLC and lyophilized. The retention time of FA-Rho was 26.5 min on PR-HPLC.

In order to verify whether the FA-GFLG-SN38 is responsive to CTSB, we applied fluorescence spectroscopy to detect the fluorescence changes of FA-GFLG-SN38 in the presence of CTSB. As shown in Figure 1A, free SN38 showed yellow native fluorescence under UV irradiation. FA-GFLG-SN38 displayed no fluorescence due to quenching of SN38 fluorescence through binding with other conjugates. Treatment of FA-GFLG-SN38 with CTSB at 37°C was characterized using fluorescence spectroscopy (Figure 1B). The fluorescence signal was not enhanced in the absence of CTSB, confirming obvious quenching of FA-GFLG-SN38. Fluorescence increased with time in CTSB solutions, which was caused by enzymatic cleavage of the tetrapeptide GFLG in FA-GFLG-SN38 and subsequent release of SN38 ($\lambda_{ex}$ = 365 nm, $\lambda_{em}$ = 540 nm). In contrast, no increase in fluorescence was observed upon treatment of FA-GFLG-SN38 with CTSB in the presence of the inhibitor CA-074 Me. These findings indicate that the SN38 is inactive when linked to the delivery system, and upon its CTSB-triggered release from the FA-GFLG-SN38, it restores its fluorescence and therapeutic activity.

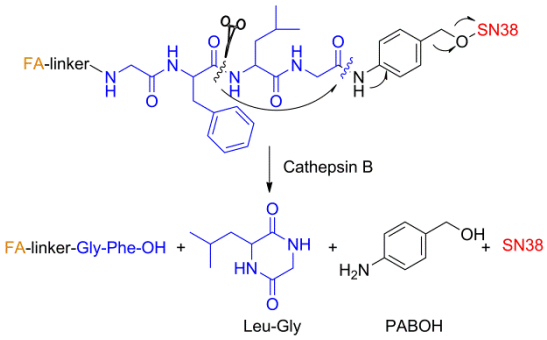


**Scheme 2.** Cleavage of FA-GFLG-SN38 by CTSB.

To further verify the CTSB-triggered release of SN38 from FA-GFLG-SN38, mixtures obtained from treatment of FA-GFLG-SN38 in the presence of CTSB were characterized and monitored using RP-HPLC and mass spectrometry. The results showed that SN38 (retention time = 23.6 min, [M + H]: m/z = 393.1) was efficiently released from FA-GFLG-SN38 (retention time = 26.4 min, [M + Na]: m/z = 1764.3) and produced along with FA-linker-Gly-Phe-OH (retention time = 21.4 min, [M + Na]: m/z = 1114.7) in the presence of CTSB (Figure 1C). Mixtures were further subjected to liquid chromatography-mass spectrometry, which revealed the presence of cyclic dipeptides (Leu-Gly: retention time = 34.0 min, [M + H]: m/z = 171.2). The tetrapeptidic substrate in FA-GFLG-SN38 was enzymatic hydrolyzed by CTSB into Gly-Phe and Leu-Gly, and the drug released via a 1,6-elimination process when the C-terminus of the dipeptide (Leu-Gly) in the delivery system was cleaved (Scheme 2). The above observations demonstrate that FA-GFLG-SN38 is cleaved by CTSB to release FA-linker-Gly-Phe-OH, cyclic dipeptide (Leu-Gly), PABOH, and SN38.

To determine the effect of FR specificity on the cellular internalization rate of the delivery system, we compared fluorescence of SK-Hep-1, A549 and 16-HBE cells immediately after incubation with FA-Rho. Rhodamine B exhibits fluorescence in both its free and conjugate forms.[35] It was expected that FA-Rho accumulation in cells would occur through FR-mediated endocytosis, followed by increased fluorescence emission in cells caused by rhodamine B localize.[36] The results of confocal microscopy analysis of the treated SK-Hep-1 cancer cells show that a red fluorescence signal is detected mainly in the lysosomes (Figure 2). After pre-incubation with CA-074 Me (20 μM) and subsequent treatment with 5 μM FA-Rho, strong red fluorescence signals were observed in SK-Hep-1 cancer cells. However, when SK-Hep-1 cells were incubated with FA for 1 h and then treated with FA-Rho, fluorescence signal associated with rhodamine

B were attenuated. The results showed that rhodamine B was enriched in cells due to endocytosis of FR. In addition, faint

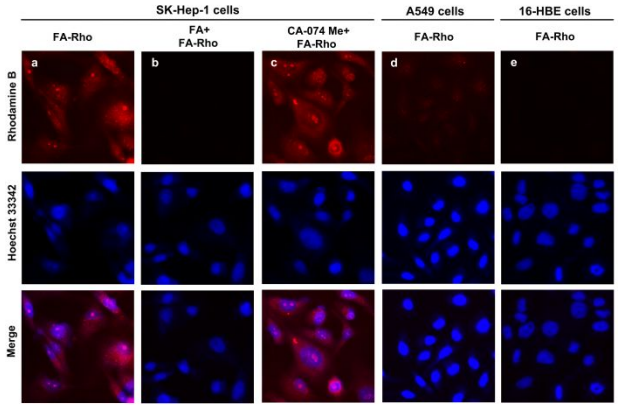


**Figure 2.** Fluorescence imaging of cells treated with FA-Rho. SK-Hep-1 cancer cells were incubated with (a) 5 μM FA-Rho for 24 h, (b) 3 mM FA for 1 h and then 5 μM FA-Rho for 24 h, (c) 20 μM CA-074 Me for 24 h and then 5 μM FA-Rho for 24 h. (d) A549 cancer cells were incubated with 5 μM FA-Rho for 24 h. (e) 16-HBE normal cells were incubated with 5 μM FA-Rho for 24 h. Hoechst 33342 (1 μg/mL) were used to stain the nucleus. The incubated cells were imaged with confocal microscopy.

fluorescence was detectable in FA-Rho treated A549 cancer cells or 16-HBE normal cells owing to low expression levels of FR. The above observations clearly suggest that the FA-Rho exerts selective fluorescence imaging on cancer cells through FR-mediated endocytosis.

The usefulness of FA-GFLG-SN38 for fluorescence detection of cancer and normal cells was investigated. Unlike rhodamine B, the fluorescence of SN38 depends on existing in its free or conjugate form, when the conjugated system was modified, the SN38-conjugate will be in its "Turn-OFF" state,[37] through enzymatically-cleavable group would transform the system into a "Turn-ON" state. We infer that if free SN38 is released from the FA-GFLG-SN38 binding under the action of lysosomal CTSB, it should accumulate in the nucleus of its action due to its fast diffusion kinetics.[38] To

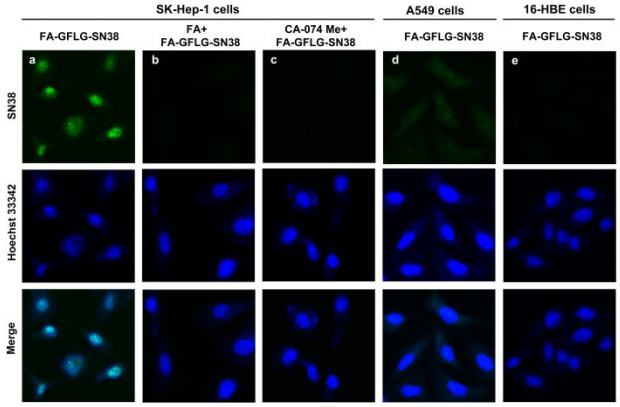


**Figure 3.** Fluorescence imaging of cells treated with FA-GFLG-SN38. SK-Hep-1 cancer cells were incubated with (a) 5 μM FA-GFLG-SN38 for 24 h, (b) 3 mM FA for 1 h and then 5 μM FA-GFLG-SN38 for 24 h, (c) 20 μM CA-074 Me for 24 h and then 5 μM FA-GFLG-SN38 for 24 h. (d) A549 cancer cells were incubated with 5 μM FA-GFLG-SN38 for 24 h. (e) 16-HBE normal cells were incubated with 5 μM FA-GFLG-SN38 for 24 h. Hoechst 33342 (1 μg/mL) were used to stain the nucleus. The incubated cells were imaged with confocal microscopy.

probe the expectations, we compared the fluorescence of SK-Hep-1, A549, and 16-HBE cells immediately after incubation with 5 μM FA-GFLG-SN38. As shown in Figure 3, strong green fluorescence was detected in nuclei of treated SK-Hep-1 cancer cells, indicating that released SN38 does indeed spread to and localize in the nucleus. However, before treatment with 5 μM FA-GFLG-SN38, the fluorescence intensity of the SK-Hep-1 cancer cells pre-incubated with 3 mM FA was significantly reduced. On the other hand, SK-Hep-1 cancer cells preincubated with CA-074 Me (20 μM) and subsequent treatment with 5 μM FA-GFLG-SN38 exhibit faint fluorescence signals. The above results indicated that although FA-GFLG-SN38 was degraded in SK-Hep-1 cancer cells, in the presence of CA-074 Me, the coupling was not cleaved by intracellular cathepsin B and released free SN38. A549 cells were incubated with FA-GFLG-SN38, faint fluorescence signals was observed in the lysosomes, phenomena which are similar to those promoted by incubation mixtures of cancer cells with FA-Rho in the presence of FA. In addition, no fluorescence was detectable in FA-GFLG-SN38 treated 16-HBE normal cells owing to lack of FR. Taken together, the results show that both FR and CTSB activity are required for the release of free SN38 from FA-GFLG-SN38 in SK-Hep-1 cells where it accumulates in the nucleus.

The anti-tumorigenic activity of FA-GFLG-SN38 was evaluated by measuring the viability of cancer (HeLa, Siha, A549, and SK-Hep-1) and normal (16-HBE) cells using the MTT assay (MTT = 3-(4,5-dimethylthiazol-2-yl)-2,5-diphenylte-trazolium bromide). It is well known that HeLa cells express FR-positive, while A549 cells are FR-negative.[39] The results indicated that FA-GFLG-SN38 had a significant anti-tumorigenic activity against SK-Hep-1, HeLa, and Siha cells with an $IC_{50}$ values of 2–3 μM (Figure 4A). FA-GFLG-SN38 reduced the cell viability of A549 cells by 51% under concentration of 20 μM, while that of 16-HBE normal cells at the same concentration decreased by 24%. The low toxicity of FA-GFLG-SN38 to A549 and 16-HBE cells is due to the deficiency of FR, which is consistent with the described phenomenon of fluorescence imaging. These results indicate preferential activity of FA-GFLG-SN38 against FR-positive cells. Next, we examined the anti-proliferative activity of free SN38 on cancer and normal cells. Free SN38 exhibited strong cytotoxic against cancer and normal cells with an $IC_{50}$ values of 0.3-1 μM (Figure 4B). These results suggest that FA-GFLG-SN38 selectively targets cancer cells containing FR and CTSB, and FA-GFLG-SN38 could be used as an effective system for targeted therapy of tumor cells. results show that both FR and CTSB activity are required for the release of free SN38 from FA-GFLG-SN38 in SK-Hep-1 cells where it accumulates in the nucleus.

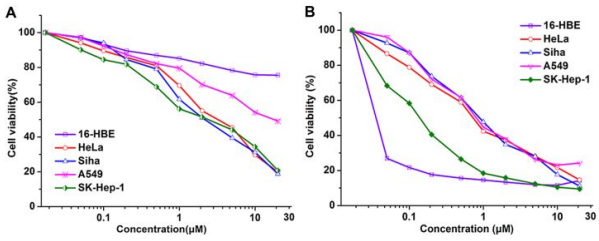

**Figure 4.** Cancer and 16-HBE cells were incubated with various concentrations of (A) FA-GFLG-SN38 or (B) free SN38 for 72 h. Cell viability was measured with the MTT assay.

In summary, we have successfully developed two FR-mediated delivery systems. FA-Rho probe is suitable for specific fluorescence imaging of SK-Hep-1 cancer cells for overexpressing FR, and usually inactive in FR negative cells (A549 and 16-HBE cells). The FR-mediated cathepsin B sensitive drug delivery system (FA-GFLG-SN38) is composed of ligand (FA) of FR, tetrapeptide substrate (-GFLG-) for cathepsin B and an anticancer drug (SN38). The experimental results showed that FA-GFLG-SN38 is an effective anti-tumorigenic agent. FA-GFLG-SN38 integrates features of enzymatically-triggered drug release, fluorescence imaging and targeted drug delivery into one system. Our preliminary studies suggest that SN38 is released from FA-GFLG-SN38 in the presence of CTSB and emits fluorescence, which can be effectively applied for cancer cells for overexpressing FR. The FA-GFLG-SN38 delivery system exhibited strong cytotoxic against SK-Hep-1, HeLa and Siha cells of $IC_{50}$ = 2–3 μM, with no effects on FR negative A549 and 16-HBE cells, thus minimizing the toxic side-effects of anticancer drugs. Based on the collective findings, we propose that the newly developed dual-targeted drug delivery system provides an effective framework for future potential applications to tumor detection and targeted therapy *in vivo*.

## ASSOCIATED CONTENT

### Supporting Information

The Supporting Information is available free of charge on the ACS Publications website.

Experimental procedures, chemical characterization, biochemical methods and additional data (PDF)

## AUTHOR INFORMATION


### Corresponding Author

*E-mail: xizhet@ybu.edu.cn and lliu@ybu.edu.cn

### ORCID

Xizhe Tian: 0000-0001-9608-1180


### Notes

The authors declare that there is no conflicts of interest.

## ACKNOWLEDGMENT

This study was supported financially by the National Science foundation of China (grant no. 21462045 and 31760330).

## ABBREVIATIONS

FR, folate receptor; FA, folic acid; SN38, 7-ethyl-10-hydroxycamptothecin; CTSB, cathepsin B; GFLG, Gly-Phe-Leu-Gly; Rho, rhodamine B; HOBt, 1-hydroxybenzotriazole; DIEA, diisopropylethylamine; PABOH, 4-aminobenzyl alcohol; DIC, *N,N′*--diisopropylcarbodiimide; TFA, trifluoroacetic acid; DCC, *N,N′*-dicyclohexylcarbodiimide; RP-HPLC, reversed-phase high performance liquid chromatography; MTT, 3-(4,5-dimethylthiazol-2-yl)-2,5-diphenylte-trazolium bromide.

## REFERENCES


1.Chen, Z. H.; Yu, Y. P.; Tao, J.; Liu, S.; Tseng, G.; Nalesnik, M.; Hamilton, R.; Bhargava, R.; Nelson, J. B.; Pennathur, A.; Monga, S. P.; Luketich, J. D.; Michalopoulos, G. K.; Luo, J. H. MAN2A1-FER Fusion Gene is Expressed by Human Liver and Other Tumor Types and has Oncogenic Activity in Mice. *Gastroenterology* **2017,** *153,*1120-1132.

2. Steinskog, E. S.; Sagstad, S. J.; Wagner, M.; Karlsen, T. V.; Yang, N.; Markhus, C. E.; Yndestad, S.; Wiig, H.; Eikesdal, H. P. Impaired Lymphatic Function Accelerates Cancer Growth. *Oncotarget* **2016,** *7,*45789-45802.

3. Ehrlich, P. Die Behandlung Der Syphilis Mit Dem Ehrlichschen Präparat 606. *Deut. Med. Wochenschr.***1910,** 1893-1896.

4. Zhang, X.; Meng, L.; Lu, Q.; Fei, Z.; Dyson, P. J. Targeted Delivery and Controlled Release of Doxorubicin to Cancer Cells Using Modified Single Wall Carbon Nanotubes. *Biomaterials* **2009,** *30,* 6041-6047.

5. Wang, Y.; Huang, Q.; He, X.; Chen, H.; Zou, Y.; Li, Y.; Lin, K.; Cai, X.; Xiao, J.; Zhang, Q.; Cheng, Y. Multifunctional Melanin-Like Nanoparticles for Bone-Targeted Chemo-Photothermal Therapy of Malignant Bone Tumors and Osteolysis. *Biomaterials* **2018,** *183,* 10-19.

6. Péraudeau, E.; Cronier, L.; Monvoisin, A.; Poinot, P.; Mergault, C.; Guilhot, F.; Tranoy-Opalinski, I.; Renoux, B.; Papot, S.; Clarhaut, J. Enhancing Tumor Response to Targeted Chemotherapy Through Up-Regulation of Folate Receptor α Expression Induced by Dexamethasone and Valproic Acid. *J. Control. Release* **2018,** *269,* 36-44.

7. Rooijen, J. M.; Qiu, S. Q.; Bosscha, H. T.; Vegt, B.; Boers, J. E.; Schröder, C. P.; Vries, E. G. E. Androgen Receptor Expression Inversely Correlates with Immune Cell Infiltration in Human Epidermal Growth Factor Receptor 2–Positive Breast Cancer. *Eur. J. Cancer* **2018,** *103,* 52-60.

8. Büll, C.; Heise, T.; Adema, G. J.; Boltje, T. J. Sialic Acid Mimetics to Target the Sialic Acid-Siglec Axis. *Trends Biochem. Sci.* **2016,** *41,* 519-531.

9. Liang, S.; Li, M.; Yu, X.; Jin, H.; Zhang, Y.; Zhang, L.; Zhou, D.; Xiao, S. Synthesis and Structure-Activity Relationship Studies of Water-Soluble β-Cyclodextrin-Glycyrrhetinic Acid Conjugates as Potential Anti-Influenza Virus Agents. *Eur. J. Med. Chem.* **2019,** *166,* 328-338.

10. Lyons, V. J.; Helms, A.; Pappas, D. The Effect of Protein Expression on Cancer Cell Capture Using the Human Transferrin Receptor (CD71) As an Affinity Ligand. *Anal. Chin. Acta.* **2019,** *1076,* 154-161.

11. Hansen, M. F.; Jensen, S.; Füchtbauer, E. M.; Martensen, P. M. High Folic Acid Diet Enhances Tumour Growth in PyMT-Induced Breast Cancer. *Br. J. Cancer* **2017,** *116,* 752-761.

12. Xu, Z.; Hou, M.; Shi, X.; Gao, Y. E.; Xue, P.; Liu, S.; Kang, Y. Rapidly Cell-Penetrating and Reductive Milieu-Responsive Nanoaggregates Assembled from an Amphiphilic Folate-Camptothecin Prodrug for Enhanced Drug Delivery and Controlled Release. *Biomater. Sci*. **2017**, *5*, 444–454.

13. Blom, H. J.; Shaw, G. M.; Heijer, M.; Finnell, R. H. Neural Tube Defects and Folate: Case Far from Closed. *Nat. Rev. Neurosci*. **2006,** *7,* 724-731.

14. Wu, Y.; Zhu, L.; Sheng, C.; Yao, J.; Miao, Z.; Zhang, W.; Wei, Y.; Shi, R. Synthesis and Biological Activities of Fluorinated 10-Hydroxycamptothecin and SN38. *J. Fluorine Chem.* **2014,** *157,* 48-51.

15. Ma, M. K.; McLeod, H. L. Lessons Learned from the Irinotecan Metabolic Pathway. *Curr. Med. Chem*. **2003**, *10*, 41–49.

16. Mosallaei, N.; Mahmoudi, A.; Ghandehari, H.; Yellepeddi, V. K.; Jaafari, M. R.; Malaekeh-Nikouei, B. Solid Lipid Nanoparticles Containing 7-Ethyl-10-Hydroxycamptothecin (SN38): Preparation, Characterization, in vitro, and in vivo Evaluations. *Eur. J. Pharm. Biopharm.* **2016,** *104,* 42-50.

17. Liu, H.; Lu, H.; Liao, L.; Zhang, X.; Gong, T.; Zhang, Z. Lipid Nanoparticles Loaded with 7-Ethyl-10-Hydroxycamptothecin-Phospholipid Complex: in vitro and in vivo Studies. *Drug Deliv.* **2015**, *22*, 701–709.

18. Tsai, M. H.; Peng, C. L.; Yang, S. J.; Shieh, M. J. Photothermal, Targeting, Theranostic Near-Infrared Nanoagent with SN38 against Colorectal Cancer for Chemothermal Therapy. *Mol. Pharm.* **2017,** *14,* 2766-2780.

19. Jin, C.; Wen, S.; Zhang, Q.; Zhu, Q.; Yu, J.; Lu, W. Synthesis and Biological Evaluation of Paclitaxel and Camptothecin Prodrugs on the Basis of 2-Nitroimidazole. *ACS Med. Chem. Lett.* **2017,** *8,* 762-765.

22. Beck, A.; Goetsch, L.; Dumontet, C.; Corvaïa, N. Strategies and Challenges for the Next Generation of Antibody-Drug Conjugates. *Nat. Rev. Drug Discov.* **2017,** *16,* 315-337.

23. Che, J.; Okeke, C. I.; Hu, Z. B.; Xu, J. DSPE-PEG: a Distinctive Component in Drug Delivery System. *Curr. Pharm. Des.* **2015,** *21,* 1598-1605.

24. Ocean, A.J., Niedzwiecki, D., Atkins, J.N., Parker, B., O'Neil, B.H., Lee, J.W., Wadler, S., Goldberg, R.M. LE-SN38 for Metastatic Colorectal Cancer after Progression on Oxaliplatin: Results of CALGB 80402. *J. Clin. Oncol.* **2008**, *26*, 4109-4109.

25. Pang, X.; Jiang, Y.; Xiao, Q.; Leung, A.W.; Hua, H.; Xu, C. pH-Responsive Polymer-Drug Conjugates: Design and Progress. *J. Control Release* **2016,** *222,* 116-129.

26. Yin, W.; Li, J.; Ke, W.; Zha, Z.; Ge, Z. Integrated Nanoparticles to Synergistically Elevate Tumor Oxidative Stress and Suppress Antioxidative Capability for Amplified Oxidation Therapy. *ACS Appl. Mater. Interfaces* **2017,** *9,* 29538-29546.

27. Dong, L.; Xia, S.; Wu, K.; Huang, Z.; Huan, C.; Chen, J.; Zhang, J. A pH/Enzyme-Responsive Tumor-Specific Delivery System for Doxorubicin. *Biomaterials* **2010,** *31,* 6309-6316.

28. Merchant, M.; Naqaraju, G. P.; Rajitha, B.; Lammata, S.; Jella, K. K.; Buchwald, Z. S.; Lakka, S. S.; Ali, A. N. Matrix Metalloproteinases: Their Functional Role in Lung Cancer. *Carcinogenesis* **2017,** *38,* 766-780.

29. Enyedi, B.; Jelcic, M.; Niethammer, P. The Cell Nucleus Serves as a Mechanotransducer of Tissue Damage-Induced Inflammation. *Cell* **2016,** *165,* 1160-1170.

30. Iacobuzio-Donahue, C. A.; Shuja, S.; Cai, J.; Peng, P.; Murnane, M. J. Elevations in Cathepsin B Protein Content and Enzyme Activity Occur Independently of Glycosylation During Colorectal Tumor Progression. *J. Biol. Chem*. **1997**, *272*, 29190–29199.

31. Chu, D. S.; Johnson, R. N.; Pun, S. H. Cathepsin B-Sensitive Polymers for Compartment-Specific Degradation and Nucleic Acid Release. *J. Control Release* **2012,** *157,* 445-454.

32. Schmid, B.; Chung, D. E.; Warnecke, A.; Fichtner, I.; Kratz, F. Albumin-Binding Prodrugs of Camptothecin and Doxorubicin with an Ala-Leu-Ala-Leu-Linker that are Cleaved by Cathepsin B: Synthesis and Antitumor Efficacy. *Bioconjuq. Chem.* **2007,** *18,* 702-716.

20. Huang, B.; Desai, A.; Tang, S.; Thomas, T. P.; Baker, J. R. Jr. The Synthesis of a c(RGDyK) Targeted SN38 Prodrug with an Indolequinone Structure for Bioreductive Drug Release. *Org. Lett.* **2010,** *12,*1384-1387.

21. Li, K.; Wang, S. Preparation, Pharmacokinetic Profile, and Tissue Distribution Studies of a Liposome-Based Formulation of SN-38 Using an UPLC-MS/MS Method. *AAPS PharmSciTech* **2016,** *17,* 1450-1456.

33. Ferber, S.; Baabur-Cohen, H.; Blau, R.; Epshtein, Y.; Kisin-Finfer, E.; Redy, O.; Shabat, D.; Satchi-Fainaro, R. Polymeric Nanotheranostics for Real-Time Non-Invasive Optical Imaging of Breast Cancer Progression and Drug Release. *Cancer Lett.* **2014,** *352,* 81-89.

34. Willibald, J.; Harder, J.; Sparrer, K.; Conzelmann, K. K.; Carell, T. Click-Modified Anandamide siRNA Enables Delivery and Gene Silencing in Neuronal and Immune Cells. *J. Am. Chem. Soc.* **2012,** *134,* 12330-12333.

35. Mascarenhas, S. C.; Gawas, R. U.; Ghosh, B. K.; Banerjee, M.; Ganguly, A.; Chatterjee A.; Ghosh, N. N. Water-Dispersible Rhodamine B Hydrazide Loaded $TiO_2$ Nanoparticles for "Turn On" Fluorimetric Detection and Imaging of Orthosilicic Acid Accumulation *In-Vitro* in Nephrotoxic Kidney Cells. *J. Nanosci. Nanotechnol*. **2018**, *18*, 8142–8154.

36. Li, H.; Lee, C. H.; Shin, I. Preparation of a Multiple-Targeting NIR-Based Fluorogenic Probe and Its Application for Selective Cancer Cell Imaging. *Org. Lett*. **2019**, *21*, 4628–4631.

37. Salmanpour, M.; Yousefi, G.; Samani, S. M.; Mohammadi, S.; Anbardar, M. H.; Tamaddon, A. Nanoparticulate delivery of Irinotecan Active Metabolite (SN38) in Murine Colorectal Carcinoma through Conjugation to Poly (2-ethyl 2-oxazoline)-b-poly (L-glutamic acid) Double Hydrophilic Copolymer. *Eur. J. Pharm. Sci*. **2019,** *136*, 104941.

38. Tian, X.; Baek, K. H.; Shin, I. Dual-Targeting Delivery System for Selective Cancer Cell Death and Imaging. *Chem. Sci.* **2013,** *4,* 947-956.

39. Xu, Z.; Shi, X.; Hou, M.; Xue, P.; Gao, Y. E.; Liu, S. Y.; Kang, Y. Disassembly of Amphiphilic Small Molecular Prodrug with Fluorescence Switch Induced by pH and Folic Acid Receptors for Targeted Delivery and Controlled Release. *Colloids. Surf. B Biointerfaces*. **2017**, *150*, 50–58.

40. Dhanasekaran, S. Augmented Cytotoxic Effects of Paclitaxel by Curcumin Induced Overexpression of Folate Receptor-α for Enhanced Targeted Drug Delivery in HeLa Cells. *Phytomedicine*. **2019**, *56*, 279–285.